

Table 2: Locations of the two-species equilibria in the four models.

Model	X_0	Y_0
3D	$\frac{1+\epsilon}{b-1}$	$\frac{bg}{b-1} \left(1 - \frac{1+\epsilon}{N(b-1)}\right)$
Full 2D	$\frac{1+\epsilon}{b-1}$	$\frac{bg}{b-1} \left(1 - \frac{1+\epsilon}{N(b-1)}\right)$
$O(\epsilon)$ 2D	$(b-1)X_0^3 + (2b - \epsilon b^2 - 3)X_0^2 + (b-3)X_0 - 1 = 0$	$\frac{bg}{b-1} \left(1 - \frac{X_0}{N}\right)$
Holling type II 2D	$\frac{1}{b-1}$	$\frac{bg}{b-1} \left(1 - \frac{1}{N(b-1)}\right)$

7.3.2 Linear stability

To analyze the linear stability of the three equilibria in all four systems, we linearize each system about an arbitrary point, (h_0, s_0, X_0) , or (X_0, Y_0) .

3D system

$$\frac{d}{dt} \begin{pmatrix} \Delta h \\ \Delta s \\ \Delta X \end{pmatrix} = \begin{pmatrix} -(\frac{1}{\epsilon}X_0 + 1) & \frac{1}{\epsilon} + b & -\frac{1}{\epsilon}h_0 \\ \frac{1}{\epsilon}X_0 & -(\frac{1}{\epsilon} + 1) & \frac{1}{\epsilon}h_0 \\ -X_0 & 0 & -h_0 + g(1 - \frac{2X_0}{N}) \end{pmatrix} \begin{pmatrix} \Delta h \\ \Delta s \\ \Delta X \end{pmatrix}$$

Full 2D system

$$\frac{d}{dt} \begin{pmatrix} \Delta X \\ \Delta Y \end{pmatrix} = \begin{pmatrix} m_{XX} & m_{XY} \\ m_{YX} & m_{YY} \end{pmatrix} \begin{pmatrix} \Delta X \\ \Delta Y \end{pmatrix}, \text{ where}$$

$$m_{XX} = g\left(1 - \frac{2X_0}{N}\right) - \left(1 - \frac{X_0}{\sqrt{(X_0+1)^2 + 4\epsilon b X_0}}\right) \frac{2(1+\epsilon b)Y_0}{1+X_0 + \sqrt{(X_0+1)^2 + 4\epsilon b X_0} + 2\epsilon b}$$

$$m_{XY} = \frac{2(1+\epsilon b)X_0}{1+X_0 + \sqrt{(X_0+1)^2 + 4\epsilon b X_0} + 2\epsilon b}$$

$$m_{YX} = \left(\frac{b}{\sqrt{(X_0+1)^2 + 4\epsilon b X_0}}\right) \frac{2(1+\epsilon b)Y_0}{1+X_0 + \sqrt{(X_0+1)^2 + 4\epsilon b X_0} + 2\epsilon b}$$

$$m_{YY} = -1 - \frac{1}{2\epsilon}(X_0 + 1 + \sqrt{(X_0+1)^2 + 4\epsilon b X_0})$$

$O(\epsilon)$ 2D system

$$\frac{d}{dt} \begin{pmatrix} \Delta X \\ \Delta Y \end{pmatrix} = \begin{pmatrix} g\left(1 - \frac{2X_0}{N}\right) - \frac{Y_0}{(1+X_0)^2} - \epsilon \frac{3bX_0^2 Y_0}{(1+X_0)^4} & -\frac{X_0}{1+X_0} - \epsilon \frac{bX_0^3}{(1+X_0)^3} \\ \frac{bY_0}{(1+X_0)^2} + \epsilon \frac{b^2(X_0^2 - 2X_0)Y_0}{(1+X_0)^4} & \frac{bX_0}{1+X_0} - 1 - \epsilon \frac{b^2 X_0^2}{(1+X_0)^3} \end{pmatrix} \begin{pmatrix} \Delta X \\ \Delta Y \end{pmatrix}$$

Holling type II 2D system

$$\frac{d}{dt} \begin{pmatrix} \Delta X \\ \Delta Y \end{pmatrix} = \begin{pmatrix} g\left(1 - \frac{2X_0}{N}\right) - \frac{Y_0}{(1+X_0)^2} & -\frac{X_0}{1+X_0} \\ \frac{bY_0}{(1+X_0)^2} & \frac{bX_0}{1+X_0} - 1 \end{pmatrix} \begin{pmatrix} \Delta X \\ \Delta Y \end{pmatrix}$$

About the origin, every linearized system has an eigenvalue of g , which is positive, so the extinction equilibrium is always unstable. Linearizing about the prey-only equilibrium, one finds that each system goes unstable according to the same parameter

inequalities that determine when the two-species equilibrium exists. This is as expected from a transcritical bifurcation; the stability of the prey-only equilibrium changes precisely when it collides with the two-species equilibrium, which is also the moment when that equilibrium becomes physical. As for the two-species equilibrium, we can study its stability analytically in the Holling type II system, but the other linearized systems are messy, so we solve their stability eigenproblems numerically.

7.3.3 Stability of the two-species equilibrium in the Holling type II 2D system

The Holling type II system linearized about its two-species equilibrium is

$$\frac{d}{dt} \begin{pmatrix} \Delta X \\ \Delta Y \end{pmatrix} = \begin{pmatrix} \frac{g}{b} \left(1 - \frac{b+1}{N(b-1)}\right) & -\frac{1}{b} \\ g(b-1 - \frac{1}{N}) & 0 \end{pmatrix} \begin{pmatrix} \Delta X \\ \Delta Y \end{pmatrix}.$$

The stability of the two-species equilibria is not hard to compute analytically for the Holling type II system. The characteristic equation of the linearized system is

$$\lambda^2 - \frac{g}{b} \left(1 - \frac{b+1}{N(b-1)}\right) \lambda + \frac{g}{b} \left(b-1 - \frac{1}{N}\right) = 0.$$

For the two-species equilibrium to exist, the $O(1)$ coefficient of the characteristic equation must be positive. Thus, solving the quadratic equation for λ , the discriminant will either be imaginary or of smaller magnitude than the $O(\lambda)$ coefficient. Either way, both eigenvalues will be negative (the equilibrium will be stable) if and only if the $O(\lambda)$ coefficient is positive, i.e. when $N < \frac{b+1}{b-1}$. When N exceeds this value, all three equilibria are unstable. We later prove that all orbits are bounded, so the Poincaré-Bendixon theorem will guarantee that the system converges to a limit cycle.

7.3.4 Bifurcations

The transcritical bifurcation occurs when Y_0 exceeds zero, which occurs when the X_0 expressions reported in Table 2 are less than N . For each system, this is possible only when $b > 1$. The exact relation between b and N at the bifurcations are given in Table 3. Note that from a point in parameter space where the prey-only equilibrium is stable, the bifurcation may be produced by increasing either b or N . The point in parameter space where the Hopf bifurcation occurs has a simple analytic expression for the Holling type II model, so this is also given in Table 3. For the other models, the N at which the Hopf bifurcation occurs was computed numerically for given values of b , g and ϵ , and some representative results are plotted in Figure 8. The 3D transcritical bifurcation depends only on b , N and ϵ , while the Hopf bifurcation depends also on g , but quite weakly so. It is clear from Figure 8 that the full 2D model captures the transcritical bifurcation perfectly, while the truncated models are inaccurate when ϵ becomes large. At the Hopf bifurcation, the full 2D model captures the 3D behavior imperfectly, but again much better than the truncated models.

7.3.5 Lyapunov stability

Each system undergoes only the two bifurcations we have studied and has no other fixed points. All that remains is to verify that in each system the orbits are bounded for all parameter values. We shall do this by the Lyapunov method for the 3D system and the Holling type II 2D system. We shall not prove boundedness for the other two systems, whose algebraic nonlinearities would make it a cumbersome task, but we can feel confident in its veracity.

Table 3: Bifurcation points of the four models. For the $O(\epsilon)$ model, X_0 is defined implicitly by the formula given in Table 2.

Model	Transcritical bifurcation	Hopf bifurcation
3D	$0 < \frac{1+\epsilon}{b-1} \leq N$	Found numerically
Full 2D	$0 < \frac{1+\epsilon}{b-1} \leq N$	
$O(\epsilon)$ 2D	$0 < X_0 \leq N$	
Holling type II 2D	$0 < \frac{1}{b-1} \leq N$	$\frac{b+1}{b-1} \leq N$

Holling type II 2D system Examining the \dot{X} equation, we see that $\dot{X} < 0$ whenever $X > N$. Thus, if $X < N$ at the initial condition, it remains true for all time. To put an upper bound on Y that is valid for all parameters, we must consider X and Y together in a Lyapunov functional.

Let $L \equiv X + \frac{1}{b}Y$. The proportionality between X and Y is chosen such that the nonlinear Holling type II terms in \dot{L} cancel:

$$\dot{L} = gX\left(1 - \frac{X}{N}\right) - \frac{1}{b}Y.$$

Our goal is to bound \dot{L} by an affine function of L , i.e. $\dot{L} \leq \alpha - \beta L$, where $\beta > 0$. This will imply that $L < \frac{\alpha}{\beta}$ for all time if it is true initially. To bound \dot{L} by such a term we must bound the quadratic X term by an affine function of X with a negative coefficient on X . Any line tangent to the parabola at $X_* > \frac{N}{2}$ will suffice, but we seek the line that minimizes $\frac{\alpha}{\beta}$, thereby providing the optimal bound on L . An arbitrary tangent line gives the bound

$$X\left(1 - \frac{X}{N}\right) \leq \frac{X_*^2}{N} - \left(\frac{2X_*}{N} - 1\right)X,$$

which induces a bound on \dot{L} ,

$$\dot{L} \leq \frac{X_*^2}{N} - \min\left\{\frac{2X_*}{N} - 1, \frac{1}{b}\right\}L.$$

Thus,

$$L < \inf_{X_* > N/2} \frac{X_*^2}{N \min\left\{\frac{2X_*}{N} - 1, \frac{1}{b}\right\}}.$$

Assuming the above infimum occurs at an X_* such that $\frac{2X_*}{N} - 1 < \frac{1}{b}$, the optimal choice of X_* in fact contradicts the assumption when $b > 1$. So, the minimum must be $\frac{1}{b}$, meaning that $X_* \geq \frac{N}{2}\left(1 + \frac{1}{b}\right) \geq N$. The bound on L then becomes

$$L < \inf_{X_* \geq \frac{N}{2}\left(1 + \frac{1}{b}\right)} \frac{bX_*^2}{N} = \frac{N}{4b}(b+1)^2.$$

Putting this in terms of X and Y , and adding the known bound on X alone,

$$X < \min\left\{\frac{N}{4b^2}(1+b)^2 - \frac{1}{b}Y, N\right\}.$$

3D system Let $L \equiv h + \alpha s + \beta X$. To make the hX terms to vanish from \dot{L} , we let $\beta = \frac{\alpha-1}{\epsilon}$, which clearly requires $\alpha > 1$ for β to be positive. Thus,

$$\begin{aligned} \dot{L} &= -\left[\frac{1}{\epsilon} + 1 - \left(\frac{1}{\epsilon} + b\right)/\alpha\right]\alpha s - h + \frac{1}{\epsilon}(\alpha-1)gX\left(1 - \frac{X}{N}\right) \\ &\leq -m(\alpha)L + \frac{1}{\epsilon}(\alpha-1)X\left[\left(g + m(\alpha)\right) - \frac{gX}{N}\right], \end{aligned}$$

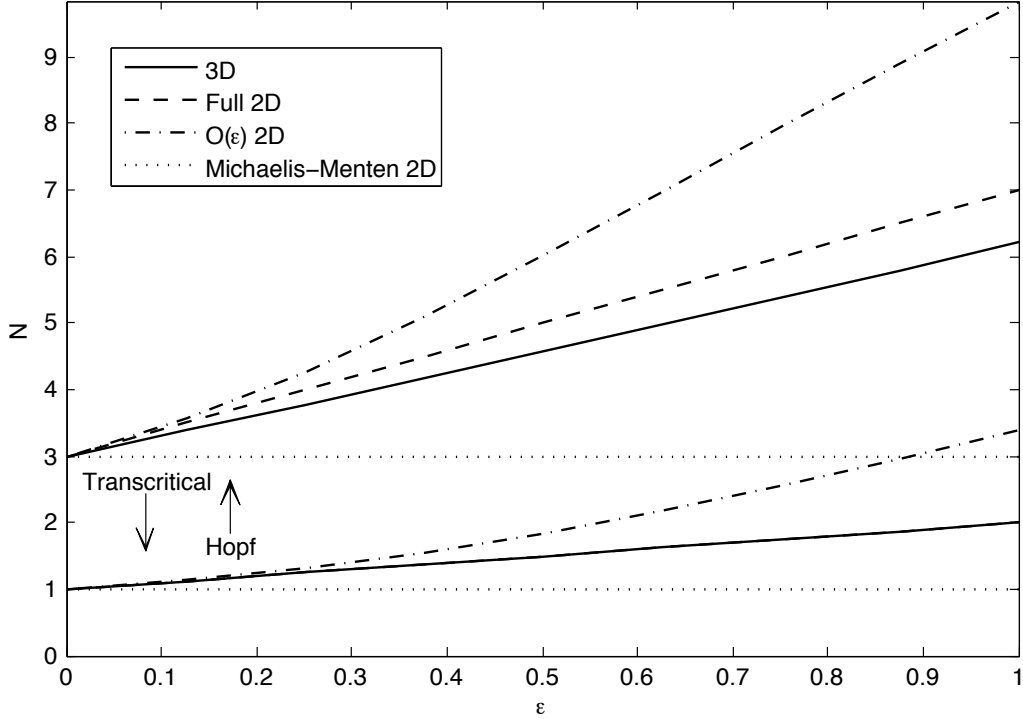


Figure 8: Values of N as a function of ϵ at the transcritical and Hopf bifurcations for all four systems with $b = 2$ and $g = 1$. For the transcritical bifurcation, the full 2D systems coincides with the 3D system.

where $m(\alpha) \equiv \min \left\{ 1, \frac{1}{\epsilon} + 1 - \left(\frac{1}{\epsilon} + b \right) / \alpha \right\}$. We now bound the quadratic X term by its maximum value without bothering to find the optimal bound linear in X .

$$\dot{L} \leq -m(\alpha)L + \frac{N}{4\epsilon g}(\alpha - 1)(g + m(\alpha))^2.$$

This yields a bound on L that can be optimized over all allowable α :

$$L < \inf_{\alpha > 1} \frac{N}{4\epsilon g} \frac{\alpha - 1}{m(\alpha)} (g + m(\alpha))^2.$$

Assuming the infimum occurs when $m(\alpha) = 1$ implies that the optimal bound is obtained by choosing $\alpha = 1^+$, which contradicts $m(\alpha) = 1$. Let $\alpha \geq \frac{1+\epsilon b}{1+\epsilon}$, giving our best result for a bound on the Lyapunov functional:

$$L < \inf_{\alpha \geq \frac{1+\epsilon b}{1+\epsilon}} \frac{N}{4\epsilon^2 g} \frac{\alpha - 1}{1 + \epsilon - \frac{1+\epsilon b}{\alpha}} \left(g + 1 + \epsilon - \frac{1+\epsilon b}{\alpha} \right)^2.$$

The optimal bound can be calculated given the other parameters, but the more important conclusion is that some such finite bound always exists for L .

7.3.6 Summary of results

Our analysis strongly suggests that X and Y have the same qualitative behavior in all four systems, though to make this result rigorous, one needs Lyapunov bounds on the

full 2D and $O(\epsilon)$ 2D systems, and one needs to show analytically that a Hopf bifurcation occurs in all systems as it does in the Holling type II system. Trusting that the systems indeed all have the same behavior, they differ only quantitatively. We have seen that the full 2D system has the same two-species equilibrium as the 3D system, while the truncated systems do not, and quantitative differences in bifurcation values were shown already in Figure 8.

Phase portraits produced by the different models appear in Figure 9. Although the 2D systems began with the same initial conditions, we must compare them each to their own corresponding 3D solution because they each correspond to slightly different decompositions of Y_0 into h_0 and s_0 . However, the three 3D solutions tend to be quite similar. The top row of Figure 9 shows solutions at small N , when the prey-only equilibrium is stable. The prey-only equilibrium is identical in all four systems, so the phase portraits agree well even for $\epsilon = 0.5$. The middle row of Figure 9 shows solutions for larger N , when the two-species equilibrium is stable. The different systems agree well when ϵ is 0.05, but at 0.5 the locations of the equilibria differ significantly, so the respective phase trajectories spiraling towards them are quantitatively quite different. The bottom row of Figure 9 shows long-time solutions at still larger N . When ϵ is 0.05, the limit cycles of the full 2D and $O(\epsilon)$ 2D systems approximate the 3D limit cycle quite well, while the Holling type II system does a bit worse. When ϵ is 0.5, the Holling type II system's limit cycle is much too large, the full 2D system's is too small but a bit better, and the $O(\epsilon)$ 2D system has not yet gone through the Hopf bifurcation.

The full 2D system approximates the 3D system well for $\epsilon \lesssim 0.5$, while the Holling type II 2D system is quantitatively accurate only when ϵ is an order of magnitude smaller. We wish to extrapolate these truths to other models where the Holling type II or full-order-in- ϵ functional forms might be used as predation laws without repeating their rigorous derivation from a higher-order dynamical system. If ϵ is very small, or if one is only concerned with qualitative features, as is often the case in biological modeling, the Holling type II functional form is certainly satisfactory. If ϵ is closer to unity, and the quantitative properties of the system matter, as is often the case in enzyme kinetics, the full-order-in- ϵ functional form would be a better choice. The $O(\epsilon)$ functional form probably offers neither enough simplicity nor accuracy to be chosen over the other two.

References

- [1] C. S. HOLLING, *Some characteristics of simple types of predation and parasitism*, Canadian Entomologist, (1959).
- [2] E. E. WERNER AND J. F. GILLIAM, *The ontogenetic niche and species interactions in size-structured populations*, Ann. Rev. Ecol. Syst., (1984).
- [3] J. P. WHITEHEAD AND C. R. DOERING, *Notes on some age structure trophic dynamics*, (2007, unpublished).
- [4] ———, *Simple hungry and satiated predator*, (2007, unpublished).

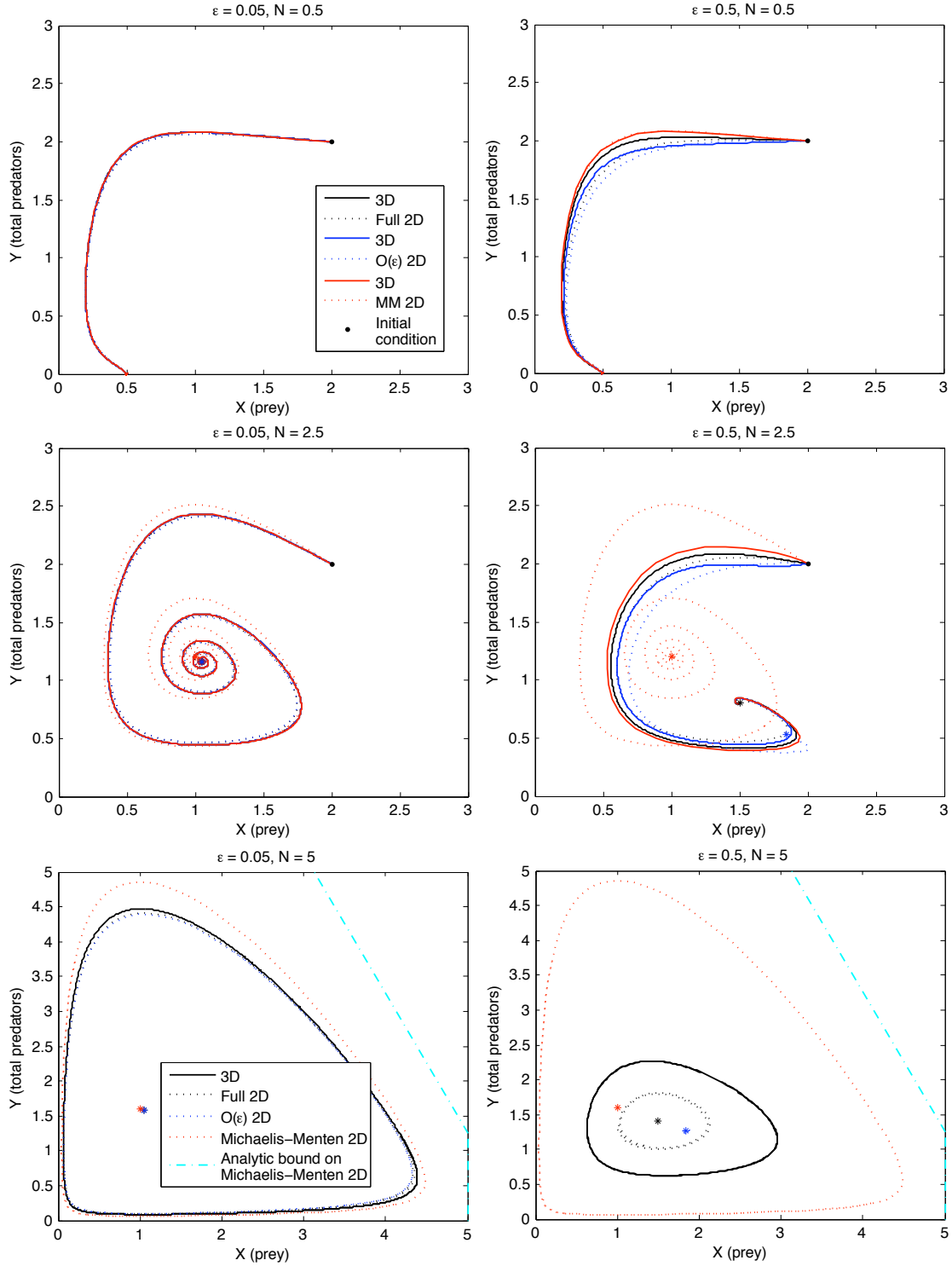


Figure 9: Phase portraits of all four systems for values of N with $\epsilon = 0.05$ (left) and $\epsilon = 0.5$ (right), and $b = 2$, $g = 1$. All solutions began at $(2,2)$, but only the late-time behavior is shown in the bottom two plots to make the limit cycles clear. The asterisks are the equilibria of the different systems, which always coincide for the 3D system and the full 2D system.